International Journal of Nanomedicine

Dovepress
open access to scientific and medical research

Open Access Full Text Article

ORIGINAL RESEARCH

Synthesis and characterization of a novel peptide-grafted Cs and evaluation of its nanoparticles for the oral delivery of insulin, in vitro, and in vivo study

This article was published in the following Dove Press journal:
International Journal of Nanomedicine

Ghullam Reza Barbari[1]
Farid Dorkoosh[1]
Mohsen Amini[2]
Nika Bahari Javan[1]
Mohammad Sharifzadeh[3]
Fateme Atyabi[1]
Saeed Balalaie[4]
Niyousha Rafiee Tehrani[5]
Morteza Rafiee Tehrani[1]

[1]Department of Pharmaceutics, School of Pharmacy, Tehran University of Medical Sciences, Tehran, Iran; [2]Department of Medicinal Chemistry, School of Pharmacy, Tehran University of Medical Sciences, Tehran, Iran; [3]Department of Pharmacology, School of Pharmacy, Tehran University of Medical Sciences, Tehran, Iran; [4]Department of Chemistry, Khajeh Nasir Toosi University, Tehran, Iran; [5]School of Medicine, Tehran University of Medical Sciences, Tehran, Iran

Background: Despite years of experience and rigorous research, injectable insulin is the sole trusted treatment method to control blood glucose level in diabetes type 1 patients, but injection of insulin is painful and poses a lot of stress to the patients, especially children, therefore, development of a non-injectable formulation of insulin is a major breakthrough in the history of medicine and pharmaceutical sciences.

Methods: In this study, a novel peptide-grafted derivative of chitosan (CPP-g- chitosan) is synthesized and its potential for oral delivery of proteins and peptides is evaluated. Drug-loaded nanoparticles were developed from this derivative using ionic gelation method with application of sodium tripolyphosphate (TPP) as a cross-linking agent. Human insulin was used as the model protein drug and release kinetics was studied at gastrointestinal pH. Finally the developed nanoparticles were filled into very tiny enteric protective capsules and its effects on blood glucose levels were evaluated in laboratory animals.

Results: Presence of the positively charged cell-penetrating peptide moiety in the structure of chitosan polymer had slight inhibitory effects on the release of insulin from the nanoparticles in simulated gastric fluid (pH 1.2) comparing to native chitosan. The nanoparticles were positively charged in gastrointestinal pH with size ranging from 180 nm to 326 nm. The polypeptide grafted chitosan is a novel analog of Penetratin, presenting both the hydrophilic and hydrophobic characteristics altering the release behavior of the nanoparticles and significantly increase the absorption of insulin into the rat epithelium comparing to nanoparticles from simple chitosan. In-vivo results in diabetic rat proved that this nanoparticulate system can significantly lower the blood glucose levels in diabetic rats and remain effective for a duration of 9–11 hours.

Conclusion: The results indicate that nanoparticles developed from this new peptide conjugated derivative of chitosan are very promising for oral delivery of proteins and peptides.

Keywords: peptide grafted, oral delivery, cell-penetrating peptide, penetratin

Introduction

Chitosan (Cs) and its growing new derivatives have been under investigation for their application in drug delivery systems. Cs is a cationic polysaccharide and a copolymer of β(1→4)-linked glucosamine and *N*-acetyl glucosamine.[1] Cs has numerous reactive amine and hydroxyl groups; therefore, the chemical modification of Cs and even further modification of its developed derivatives are possible to obtain a new derivative with the desired characteristics. A large number of different derivatives including hydrophilic, hydrophobic, thiolated, acylated, and PEGylated are reported and investigated.[2–4] Cs has some unique

Correspondence: Morteza Rafiee Tehrani
Department of Pharmaceutics, School of Pharmacy, Tehran University of Medical Sciences, North Kargar St., Tehran, Iran
Email rafitehr@ams.ac.ir

submit your manuscript | www.dovepress.com
Dovepress
http://dx.doi.org/10.2147/IJN.S161240

biological properties such as biocompatibility, biodegradability, nontoxicity, and antibacterial and antiviral activities.[5,6]

Cs is degraded by lysozyme enzyme available in various mammalian tissues leading to the production of *N*-acetyl-D-glucosamine and D-glucosamine, which in turn play important physiological roles in biological processes.[7] Due to the favorable biological properties of Cs, it is gaining more attention in pharmaceutical and biomedical studies.[8,9] In addition to other useful characteristics of Cs such as biocompatibility and biodegradability, one of the unique characteristics of Cs is its potential to open intercellular tight junctions;[10,11] this property is making Cs a promising excipient in formulations targeted for the oral delivery of proteins, peptides, and other macromolecules. Among all the peptide and protein medications, insulin has been most frequently investigated for oral delivery due to its significant effects on the health and well-being of millions of diabetic patients around the world, on the one hand, and its currently painful method of administration (injection), on the other hand.[12,13] The oral delivery of insulin is a preferred method of administration because of the following reasons: First, patient compliance is absolutely higher; second, it is more convenient to administer, and patients adhere to the therapy better compared with the painful, invasive method of injection; and third and more importantly, the oral delivery of insulin is the only route of administration that potentially mimics the physiologic insulin secretion and metabolism pathway,[14] therefore less chance of hypoinsulinemia in treated patients and its consequent complications such as nephropathy and neuropathy.[15] Although the oral delivery of insulin is preferred from different points of views, it faces some fundamental challenges, two of them are the harsh and degrading enzymatic situation of gastrointestinal track that leads to inactivation of insulin very fast and the mucosal barrier that limits insulin's final bioavailability.[16,17] Several innovative approaches have been undertaken to resolve the enzyme barrier with some of them achieving promising results.[18–20] Unfortunately, to date, there has been no successful development in resolving the mucosal barrier, which is the main reason for the failure of oral insulin formulations. To circumvent the mucosal barrier, several approaches have been undertaken, including the application of mucoadhesive nanoparticulate systems, mucoadhesive composites,[19,21,22] nanoemulsions, double emulsions, chemical modifications of insulin molecule such as acylation and PEGylation to alter hydrophobic/hydrophilic balance of insulin,[11] and the application of cell-penetrating peptides (CPPs) in both chemical[23] and physical conjugations (coadministration).[24]

CPPs, also known as protein transduction domains,[25] are small peptides (usually containing <30 amino acids), attracting most attention in the recent three decades, and their application is increasingly growing for noninvasive delivery of peptides or other macromolecules.[26] CPPs are believed to be new and powerful tools for drug delivery into the cells of all organs in a tissue-independent manner as well as trafficking inside the cells and finally resolving the cell barrier. Investigations at the levels of cell culture and animal studies have shown that covalently[23] and even physically linking a CPP (eg, TAT) to almost any type of medicine, including hydrophilic compounds and large proteins (molecular weight [MW] >150 kDa), facilitates translocation of the attached species into the cells of all organs, including the brain.[27]

In this innovative study, a novel peptide-grafted derivative of Cs (CPP-g-Cs) was developed through the chemical attachment of a polypeptide sequence (CPP) to some of the numerous amine groups of Cs. Although the synthesis of this novel derivative of Cs and fabrication of insulin-loaded nanoparticles (NPs) from this polymer, cell membrane barrier was overridden both through tight-junction-opening capabilities of Cs and more importantly direct penetration and transcytosis properties of a very potent and newly developed CPP, a novel analog of penetratin (containing 16 amino acids).[28] The CPP sequence was chemically conjugated to some of the numerous amine groups of Cs, leading to a very novel CPP-g-Cs.

Materials and methods

Materials

Medium MW Cs (75 kD) and 90% deacetylated were supplied from Primex (Siglufjordur, Iceland). *N*-hydroxysuccinimide and *N*-ethyl-*N*′-(3-dimethylaminopropyl) carbodiimide were purchased from Merck KGaA (Darmstadt, Germany). Dialysis bag (MW =12,000 Da) was purchased from Sigma-Aldrich Co. (St Louis, MO, USA). Regular human insulin United States Pharmacopeia (recombinant; rh-Insulin =28.9 IU/mg) was a gift from Ronak Ltd. (Tehran, Iran). Gelatin capsules number 9 (Braintree Inc., MA, USA). Eudragit® L100-55 was obtained from Evonik Inc. (Darmstadt, Germany). Human Insulin enzyme-linked immunosorbent assay (ELISA) Kit was procured from Alpha Diagnostic (San Antonio, TX, USA).

Methods

Synthesizing the CPP with special amino acid sequence

The CPP that we were interested to attach with Cs polymer and make a new CPP-g-Cs and to study its effect on physicochemical properties of Cs as well as its cell permeation properties is a

newly developed and different analog of the famous and well-established CPP, penetratin, which was produced and purified in our previous study.[23] Cell permeation and cargo delivery capabilities of penetratin are reported by many scientists (although with different extents) involved in the fields of cell permeation and peptide delivery.[24] Following some interesting results reported for a special analog of penetratin in an intranasal insulin delivery application (a physical mixture formulation),[29] the 16-amino acid peptide with the same amino acid sequence was synthesized in our peptide laboratory in Khajeh Nasir Toosi University and purified to >95% purity.[23] Table 1 shows the amino acid sequence of penetratin and the newly developed analog of penetratin studied in this research. In order to attach the CPP sequence to free amine groups of Cs as well as to preserve the CPP configuration after grafting to Cs, a very short-chain (9 carbon atoms) polyethylene glycol (PEG) with a free carboxylic acid at one side is attached to the N-terminus of the CPP sequence at the time of CPP synthesis.

Synthesis of the CPP-g-Cs

The polypeptide sequence, CPP, is attached to Cs polymer through the formation of the amide bond between the carboxyl group at the end of the PEG linked to CPP and some amine groups of Cs. To avoid the possible amide reactions (ri[illegible] mation) between the carboxyl group at the C-terminus of CPP and the amine groups of lysine amino acids in the struc[illegible] of CPP at the time of activation, fluorenylm[illegible]thylox[illegible]carbon[illegible] (Fmoc) protecting group is used to pro[illegible]t amin[illegible]ps in a very environmental friendly and effective [illegible]hod,[30] prior to the exposure of CPP carboxyl g[illegible]p to primary [illegible]mine groups of Cs. After amine groups a[illegible]e prote[illegible]ed, the CPP sequence is separated from the un[illegible]acted 9-fluore[illegible]dmethoxycarbonyl chloride and purifie[illegible] via a s[illegible]mipreparative reverse-phase high-performance l[illegible]id ch[illegible]matography (HPLC) method.[31]

The amin[illegible]protecte[illegible]CPP seq[illegible]nce is covalently grafted to some [illegible] the nu[illegible]erous [illegible]ine groups of Cs using carbodiimid[illegible]chemis[illegible]g follows: Fmoc-CPP sequence was solubilized[illegible]distilled water (60 mg/mL), completely mixed with *N*-hydro[illegible]succinimide (40%, w/w) and *N*-ethyl-*N*′-(3-dimethylamino)propyl carbodiimide (60%, w/w), and kept stirred for 2 hours at room temperature (RT). The aqueous solution of Cs (15 mg/mL) was added to the reaction mixture and stirred at RT for 20 hour. This overnight conjugation scheme provides the required time for chemical attachment between carboxyl groups of CPP and amine groups of Cs and the formation of a novel Cpp-g-Cs. The developed Cpp-g-Cs was dialyzed extensively against distilled water for 3 days in dialysis bags with MW cutoff point of 12,000 Da and lyophilized. Figure 1 shows the structure of Cs, the novel derivative of Cs, and the chemical conjugation process. The collected dialyzed sample wa[illegible]d for the estimation of unbound CPP sequence u[illegible]ng HPLC[illegible]nd respective linear fitting curve establish[illegible] for the CP[illegible] sequence at λ_{max}=214 nm. After chem[illegible]al conj[illegible]ation of [illegible]moc-protected CPP sequences to C[illegible] polymer, the [illegible]oc-protected amine groups of CPP (now [illegible] the [illegible]ructure of Cs) were deprotected

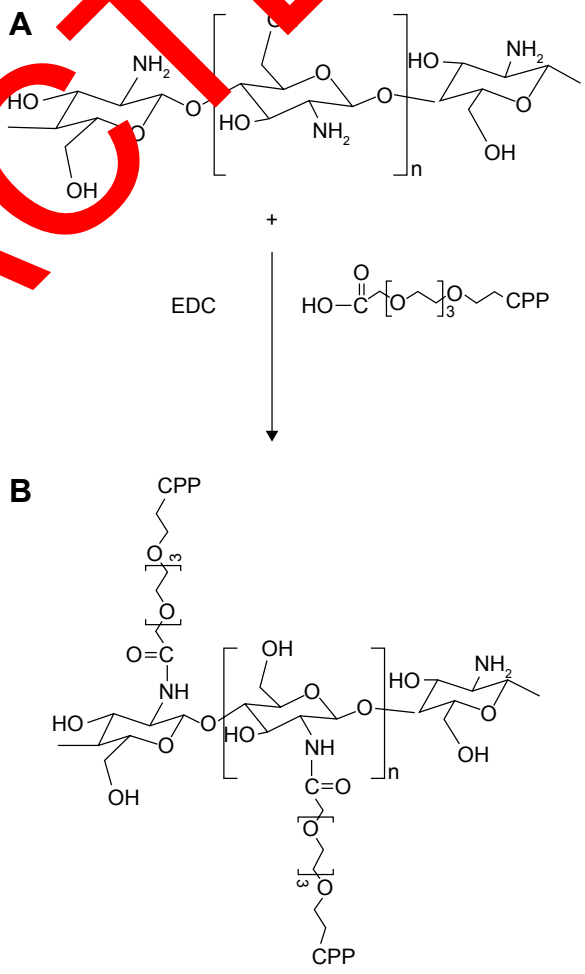

Figure 1 Chemical structure of chitosan (**A**), the novel peptide-grafted derivative of chitosan (**B**) and the schematic representation for the chemical attachment of CPP sequence to the amine groups of chitosan resulting in a novel peptide-grafted derivative of chitosan.
Abbreviations: CPP, cell-penetrating peptide; EDC, *N*-ethyl-*N*′-(3-dimethylaminopropyl) carbodiimide.

Table 1 Amino acid sequence of penetratin and its newly developed analog (PenetraMax)

Name	Sequence
Penetratin	RQIKWFQNRRMKWKK
PenetraMax	KWFKIQMQIRRWKNKR

Note: The newly developed analog (PenetraMax) consists of the same 16 amino acids as the native penetratin, but the sequence of the amino acids is manipulated to give new characteristics to PenetraMax.

in a mild and environmental friendly method according to a published protocol.[32]

Characterization of the CPP-g-Cs

Fourier transform infrared (FTIR) spectroscopy

FTIR spectra were collected from Spectrum Two spectrometer (PerkinElmer Inc., Waltham, MA USA) equipped with an accessory of a single-diamond attenuated total reflectance with the range of 550–4,500 cm^{-1} and interferometer with variable speeds of 0.1, 0.2, 0.5, 1, 2, and 4 cm/s. Infrared (IR) beam diameter is from 2 to 11 mm. IR spectra collection was performed 16 times (resolution was 4 cm^{-1}) and analyzed using Spectrum software. Cs was analyzed both before and after derivatization with the polypeptide, and the signal assignation was analyzed to investigate the successful derivatization.

^{1}H nuclear magnetic resonance (^{1}H NMR)

High-resolution ^{1}H NMR spectra were recorded from Bruker (400 MHz, AVANCE™, Billerica, MA, USA) ultra-shielded standard-bore magnet equipped with a 5 mm Broad Band Fluorine Observation probe and a Bruker Sample Case autosampler with 24 positions. Both native Cs and CPP-g-Cs were investigated to confirm structural modification in Cs. Samples were prepared dissolving 4 mg of native Cs and the new polymer in 2% deuterium chloride/D_2O mixture. The solution was heated to 60°C to ensure that the solubility is complete. Results were analyzed with Advanced Chemistry Development lab software for spectra collection and peak assignment.

Preparation of insulin-loaded NPs from CPP-g-Cs polymer

NPs from the CPP-g-Cs as well as native Cs were fabricated according to a published method. Chen et al,[32] based on the ionic gelation using three polyphosphates as a cross-linking agent to cross-link the positively charged chains of Cs. The development of the insulin-loaded NPs was carried out as follows: the CPP-g-Cs polymer was dissolved (1 mg/mL) in aqueous solution containing acetic acid (2%, w/w) and stirred for 2 hours at RT. The pH of the solution was about 4.2. The pH value was adjusted to 5.5 with the addition of a minimal amount of NaOH solution (2 M). The new CPP-g-Cs was easily and completely dissolved in acidic condition, leading to a clear solution with a slight yellow color. The polymer solution was kept stirring at RT. In another beaker, regular human insulin was dissolved in distilled water with a concentration of 2 mg/mL, and the pH of the insulin solution was adjusted to 5.5 with the addition of a minimal amount of 1 M HCL solution. After that, 2 mL of insulin solution was added dropwise to the equivalent volume of CPP-g-Cs solution and kept stirring at RT. In a separate beaker, sodium tripolyphosphate was dissolved in distilled water with a concentration of 1 mg/mL. Finally, 1 mL of three polyphosphates solution was added dropwise to 4 mL of a mixture of insulin and polymer, and the opalescent suspension was kept stirring (800 rpm) for 4 hours at RT. The insulin-loaded developed NPs were centrifuged at 15,000 rpm for 20 minutes. The obtained NPs were washed with deionized water and resuspended in distilled water to be used for size and zeta potential assessment or to be lyophilized and kept for next stage studies including drug release and in vivo studies. The same procedure was applied to produce the same insulin-loaded NPs from native Cs to perform the comparative tests to investigate the effect of peptide graft on the Cs chain.

Particle size and zeta potential studies

The particle size and zeta potential of the insulin-loaded NPs developed from both native Cs and the CPP-g-Cs were determined using dynamic light scattering (DLS) with Zetasizer Nano ZS (Malvern Instruments, Malvern, UK).

Scanning electron microscopy (SEM) studies

To investigate the particle size and the surface morphology of the insulin-loaded NPs, SEM was carried out for both the NPs from native Cs and the CPP-g-Cs. To prepare the sample for SEM studies, 6–8 µL of extra diluted sample was dropped on a piece of a completely clean glass slide and dried at RT. Then, the samples were attached to the stub and sputter-coated with a very thin layer of gold (under vacuum condition) to neutralize the charging effects prior to the start of the SEM experiment (Hitachi Ltd., Tokyo, Japan) with an acceleration voltage of 5 kV.

Encapsulation efficiency (EE) and loading efficiency (LE) studies

To determine the EE% and LE%, the exact amount (20 mg) of drug-loaded NPs from both the native and the CPP-g-Cs was dispersed in distilled water, the opalescent suspension was centrifuged at 15,000 rpm for 10 minutes at 4°C, and the supernatant was analyzed for the determination of nonencapsulated insulin using HPLC method. The samples were injected to Agilent® 1260 infinity equipped with 1260 QuatPump Vertical In-line, 1260 ALS auto sampler, and 1260 DAD VL detector. The detector was set at 214 nm. C18 column was used for HPLC analysis of insulin using linearly regressed calibration curve. The mobile phase was

a mixture of buffered aqueous phase and acetonitrile in a ratio of buffer/acetonitrile (70:30). Buffer was prepared from KH_2PO_4 (0.1 M) and triethylamine (1%), and the pH was adjusted to 2.8 using phosphoric acid. Flow rate was adjusted to 0.5 mL/min, and the data were captured using Agilent ChemStation® software (Santa Clara, CA, USA).

To calculate the EE and LE, the amount of nonencapsulated insulin in the supernatant of the centrifuged drug-loaded NPs suspension was determined. All experiments were done in triplicate, and the mean values were used to calculate the EE% and LE% according to Equations 1 and 2, respectively.

$$EE\% = \frac{\text{Total amount of insulin} - \text{Insulin in the supernatant}}{\text{Total amount of insulin}}(100) \quad (1)$$

$$LE\% = \frac{\text{Total amount of insulin} - \text{Insulin in the supernatant}}{\text{Total weight of drug} - \text{Loaded NPs}}(100) \quad (2)$$

In vitro drug release studies

To investigate the plausibility of the developed nanoparticulate system for the oral delivery of insulin and po[ssibly] a vast range of peptides and proteins, more relevantly [the] rate and extent of the release of the model peptide (i[nsulin] w[as] investigated in simulated gastric fluid (SG[F]; pH [1.2]), simulated intestinal fluid (SIF; pH 6.8, duo[denal] pH [buffer] and PBS (pH 7.4, colon pH). To study the in vitro re[lease] behavior of insulin from these NPs, prope[r] amount of ly[o]philized NPs equivalent to 20 mg of insu[lin] was [dis]persed in 900 mL of SGF, shaking at 50 rpm. The temperat[ure] was set constant at 37°C±0.5°C. The release medium was chosen relatively large to ensure the sink condition. At predetermined time intervals, spe[cific] aliquots (5 mL) were collected and replaced by a pre[-]eated b[lank] medium. The samples were centrifuged at 1[4,000] rpm for 20 minutes. The supernatant was inves[ti]ed for insulin content, and the sediment was dispersed in 1 mL blank medium and returned to release medium instead of the addition of blank medium after withdrawal of aliquots so that unreleased insulin in the withdrawn NPs is also released, because insulin release from the polymeric mesh of the NPs is not completed in the first few hours. The amount of insulin in the supernatant was determined using HPLC method as mentioned. After 2 hours, the pH of the medium is changed from 1.2 (SGF) to 6.8 (SIF) by dropwise addition of 2 mM NaOH solution and monitoring the pH. Release condition remained the same for 3 hours in pH 6.8, and then, pH is again increased to 7.4 (colon pH) with the addition of a minimal amount of 2 mM NaOH solution.

To determine the mechanism of peptide release from the developed nanoparticulate delivery system, the in vitro insulin release data were fitted to Ritger–Peppas model:

$$\frac{M_t}{M_\infty} = Kt^n \quad (3)$$

where M_t and M_∞ are the cum[ulative] release [of] insulin at time (t) and infinite time, respe[ctively], [K] is a consta[nt] related to the structural and geomet[rical] characteri[stics] [of] the device, and n is an exponent refl[ecting] the [dif]fusion mechanism. Depending on the amo[unt] of t[he] calculated values for n, the release mechanism [is] categorized. Ac[cor]dingly, if n=0.45, release mechan[ism] is [Fi]ckian (case I) diffusion; if 0.45<n<0.89, release mechanism [is] non-Fickian (anomalous) transport; and if n=0.89, release mechanism is diffusion and zero-order (case II) tran[sport].

In vi[tro] studies

[Ma]le Wistar rats (180–200 g) were obtained from the Tehran University of Medical Sciences (Tehran, Iran). The animals were housed at RT of 24°C±2°C with 12 h light/dark cycle and 40%–50% relative humidity. The animals had ad libitum access to a standard chow diet and water except, otherwise indicated. After randomization into various groups (n=6), the animals were acclimatized for a period of 2 days in the new environment, before the initiation of the experiment. The protocol for animal studies was approved by Tehran University of Medical Sciences Ethics Committee for the Rights of Laboratory Animals; the study was carried out in accordance with the principles of Laboratory Animals Rights and Care.

Induction of diabetes

For induction of diabetes, streptozotocin was administered intraperitoneally at a dose of 40 mg/kg in 0.1 M citrate buffer (pH 4.0). Blood was withdrawn from tail veins into a centrifuge tube containing EDTA and centrifuged at 80,000 rpm for 10 minutes. Plasma glucose levels were estimated using Human Insulin ELISA Kit (Alpha Diagnostic). Animals showing blood glucose levels >350 mg/dL were considered diabetic.

Oral administration of drug-loaded NPs to investigate its efficacy on blood glucose level in diabetic animals

Diabetic animals were divided (randomly) into groups of six animals each. In all the experiments including the test and control groups, animals were fasted for 1 hour before the administration of the drug delivery system as well as 1 hour after administration. The lyophilized insulin NPs from both the native Cs and the CPP-g-Cs were filled (30 IU/kg) into very tiny gelatin capsules designed for oral administration studies in laboratory animals, especially rats and Guinea pigs (capsule number 9; Braintree Inc.), enteric-coated securely via dip coating method using Eudragit L 100-55, according to a published protocol,[33] and tested and proven for efficiency of successful enteric coating (data not shown). Capsules were administered orally through especial gavage instrument. Simple solution of insulin given to one of the control groups was administered using bulb-tipped gavage needle. Control groups include insulin-loaded NPs from native Cs. Another experimental group had subcutaneous (SC) administration of 5 IU/kg plain insulin solution. Blood samples were collected at prescheduled time intervals, and plasma glucose levels were determined using glucometer (Accu-Chek, Roche, Germany). The percent change in t plasma glucose levels was calculated by designating th 0 h plasma glucose level as control value. Each group had six animals, and the results are expressed as ean v ue ± standard errors (SEs). The area under the urve (A C) of different treatments was calculated u g pl glucose concentration vs time profile with a ncompartm t-based pharmacokinetic software and relati pharmacological availability% (PA) was cal ated as foll s:

$$PA = \frac{AU\ oral \times \text{ose SC}}{AUC\ S\ \text{Dose o}} \times 100. \quad (4)$$

Statistical a lysis

All the values w expressed as mean ± SE, n=6. The significance level was de mined by one-way analysis of variance following Tukey's post hoc test. $P<0.05$ was considered as significant.

Results and discussions

MW of Cs polymer has fundamental effects on its solubility, drug loading, drug release, and size and zeta potential of the NPs developed from the polymer. According to our previous report,[23] medium- to low-MW Cs shows better properties in respect to solubility, drug loading, and release behaviors; low- or medium-MW Cs shows better properties in derivatization and more yield in chemical modifications;[34] therefore, we used medium-MW Cs (75 kDa) in this study. On the other hand, size and physicochemical properties of graft moiety have crucial effects on the final characteristics of the derivatized polymer. We successfully grafted a polypeptide sequence with 16 amino acids (Table 1) with very good water solubility and positive charge to some of the numerous amine groups of Cs. The short-chain PEG linker has some important roles, including increasing water solubility of both the CPP tag and derivati d Cs and providing a suitable space between the tag a the poly r chain so that the biological properties of C can be pres ved after chemical attachment to the ymer b kbone.

FTIR

Comparative FTIR spect both na e Cs and the new CPP-g-Cs are sh yn in Figu 2. Fi re 2A shows the three characteristi peak f Cs: 1,050 m^{-1} is related to pyranose ring in the structure o s, 1,541 cm^{-1} is related to amines of C and 1,630 cm^{-1} is related to amides remaining in the ondeacetyla d units of Cs. Figure 2B shows the two char teristic pe ks of 1,062 and 1,542 cm^{-1} related to pyranos nd e ine groups, respectively, but the appearance o w peak in 1,645 cm^{-1} shows the formation of amide b nd in the structure of Cs, suggesting successful attachment of carboxyl-terminated CPP to the amine groups of s. V_{max}/cm^{-1} 2,916 is related to (C–H stretching) of PEG in the structure of CPP used as short linker confirming the attachment of PEG containing CPP to Cs polymer. In Figure 2A and B, the area between 3,100 to 3,280 is related

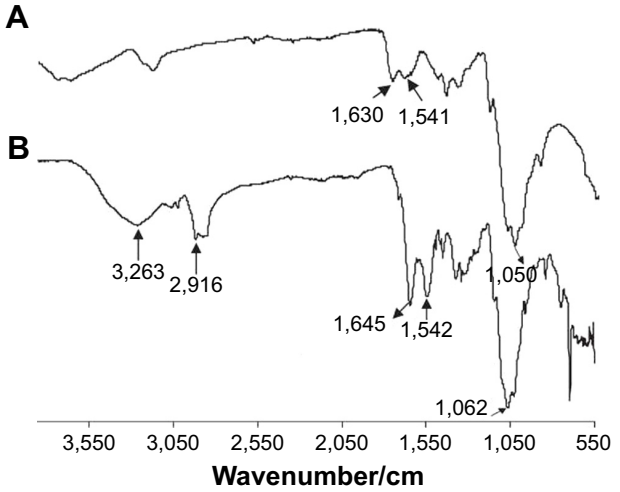

Figure 2 FTIR spectra of native chitosan (**A**) and the new peptide-grafted derivative of chitosan (**B**).
Abbreviation: FTIR, Fourier transform infrared.

to O–H groupsin the pyranose ring available in both Cs and the newly developed CPP-g-Cs.

^{1}H NMR

Figure 3 shows the comparative ^{1}H NMR spectra of native Cs and the new CPP-g-Cs. ^{1}H NMR studies reveal the successful attachment of the peptide sequence to the polysaccharide structure of Cs polymer (Figure 3). The chemical shift at δ 7.9 is related to the aromatic protons of the phenylalanine moiety in the structure of CPP confirming the presence of CPP in the structure of Cs-PEG-CPP. The multiple peaks of oxymethyl groups in PEG at δ 3.3–3.7 cover the signals from pyranose ring in the structure of Cs in Cs–N–CONH–PEG–CPP confirming the presence of PEG in the structure of Cs, implying the successful covalent attachment of PEG-terminated CPP to Cs. The peaks at δ 2.5–3.1 belong to the protons of $-CH_2-NH-NH-NH_2$ of arginine groups in the structure of CPP, and the multiple peaks at δ 1.1–1.4 are from the $-CH_2-CH_2-CH_2-NH-NH-NH_2$ in arginine in the structure of CPP conjugated to Cs. The amount of ligand attached to the NPs is quantified by the determination of the residual unreacted CPP in conjugation medium. With these calculations, the amount of CPP conjugated to the Cs is found to be 9.3% (w/w) the novel Cs derivative.

Particle size and zeta potential

The average particle sizes for drug-loaded NPs from Cs and CPP-g-Cs reported by DLS are 430± and 3 nm, respectively, with zeta potentials and meV for NPs from Cs and CPP-g-Cs, respectively.

SEM

The insulin-loaded NPs from CS and CPP-g-Cs are morphologically characterized using SEM. As shown in Figures 4 and 5, both the drug-loaded NPs developed from either Cs or CPP-g-Cs have a smooth surface and spherical shape, but their average particle sizes are different. The average particle sizes for drug-loaded NP from Cs and CPP-g-Cs are 350 and 180 nm, respectively. NPs from Cs are more aggregated and tend to bind to each other to form larger particles. Aggregation of Cs NPs is commonly seen in most reports.[35,36] Interestingly, NPs developed from the CPP-g-Cs are less aggregated and tend to stay separately. This phenomenon in comparison with NPs from the native Cs can be attributed to the presence of the positively charged polypeptide sequences in the structure of CPP-g-Cs NPs that prevent the NPs from binding to each other and aggregation.

In our previous study[35] we fabricated the same spherical NP with a smooth surface morphology, but the particle size in that study was much smaller than that in the current study. The difference in particle size may be due to the different method used for the fabrication of NPs; however, the particle size observed in SEM study was found to be smaller compared with those obtained from DLS analysis. This may be attributed to the higher hydrodynamic diameter of freshly prepared NPs measured by DLS, whereas SEM images can nullify the swelling effects.

In vitro release profile of insulin from the insulin-loaded NPs

Figure 6 shows the in vitro release profile of insulin from the NPs developed from Cs and the CPP-g-Cs by the ionic

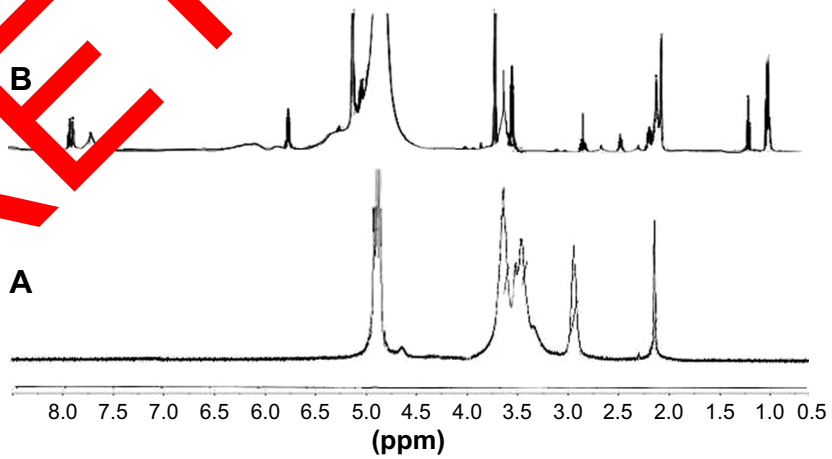

Figure 3 ^{1}H NMR spectra of both Cs and CPP-PEG-Cs confirming successful covalent conjugation with CPP; (**A**) native Cs, (**B**) peptide-grafted derivative of Cs (CPP-PEG-Cs).
Notes: The chemical shift at δ 6.7–8.2 belongs to the aromatic protons of the phenyl alanine moiety, which is present in the structure of CPP conjugated to Cs (**B**); multiple peaks of oxymethyl groups in PEG at δ 3.3–3.7 cover the signals of protons related to pyranose ring of Cs in spectra (**A**). The characteristic peak at δ 2.05 is related to protons of methoxy groups of Cs as seen in both spectra. The multiple peaks at δ 1.1–1.4 in spectra (**B**) are from the $-CH_2-CH_2-CH_2-NH-NH-NH_2$ in arginine amino acid in the CPP.
Abbreviations: CPP, cell-penetrating peptide; Cs, chitosan; ^{1}H NMR, ^{1}H nuclear magnetic resonance; PzEG, polyethylene glycol.

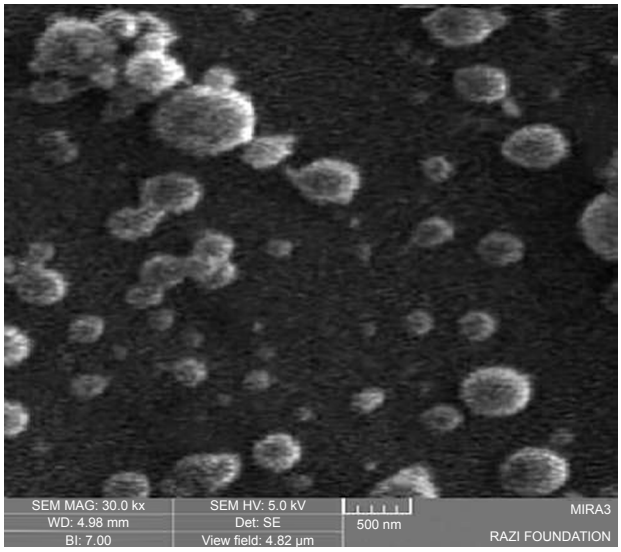

Figure 4 SEM image of insulin-loaded nanoparticles from native chitosan; size distribution is between 100 and 450 nm.
Abbreviation: SEM, scanning electron microscopy.

gelation method.[37] Release profile was investigated at three different pH values: SGF (pH 1.2), SIF (pH 6.8), and PBS (pH 7.4, colon pH). As shown in Figure 6, for both kinds of NPs, there is a burst release of insulin in the first 60 minutes in pH 1.2 (about 63% and 47% for Cs or CPP-g-Cs NPs, respectively). Then, the release of insulin continues slowly till 12 minutes when the pH of the environment is increased to 6.8. Then, the release of insulin approximately stops for NPs made of Cs when pH is increased to 6.8 (for 3 hours) as well as to the end of the dissolution time when pH is increased to and

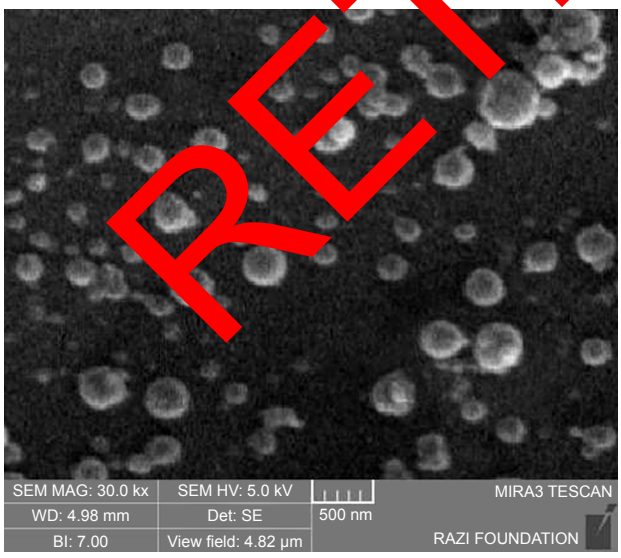

Figure 5 SEM image of insulin-loaded nanoparticles from peptide-grafted derivative of chitosan; size distribution is between 120 and 250 nm.
Abbreviation: SEM, scanning electron microscopy.

remained at 7.4 (7 hours). NPs from CPP-g-Cs also show a significant burst release of ~50% at pH 1.2 during the first 120 minutes. Insulin release from CPP-g-Cs NPs significantly slows down but continues steadily in either pH 6.8 or pH 7.4 till 9 hours, and ~83% of the drug is released. The fast and high amount of insulin release from the Cs and CPP-g-Cs NPs in pH 1.2 is due to the pH-dependent solubility of Cs that dissolves completely in acidic condition, and the NPs disintegrate and release the embedded drug. Cs has numerous amine groups that can be protonated and take positive electric charge in acidic medium making it water-soluble, and NP swells and disintegrates rapidly, resulting in the fast release of embedded drug.

Grafting the positively charged and highly water-soluble polypeptide (CPP) to the Cs backbone increases its water solubility and makes its water solubility pH-independent. As shown in Figure 6, for NPs made of native Cs, release of insulin stops at pH 6.8 and pH 7.4. This phenomenon can be attributed to shrinkage of polymer network in higher pH and insolubility of Cs in pH >6.6.[38] Interestingly, for NPs fabricated from CPP-g-Cs, primary burst release in the pH 1.2 is significantly lower than that of NPs from native Cs in spite of higher water solubility of the new CPP-g-Cs. The slower drug release from the new derivative can be attributed to the presence of positively charged polypeptide groups in the structure of polymer and more condensed polymer network absorbing and holding insulin more tightly through electrostatic or van der Waals forces. As far as the water solubility of the new derivative is pH-independent and NPs continue to disintegrate in neutral pH, release of the embedded drug from the NPs continues until most of the embedded insulin is released from the NPs, leading to around 83% release in 9 hours.

The exact mechanism of drug release from erodible, hydrophilic polymer matrices is not fully elucidated yet, and it seems to be a very complex process,[39] because different factors are playing role in this process; these include 1) permeation of water into the polymeric structure; 2) solubilization and/or erosion of the polymeric formulation; and 3) swelling of the polymer and distribution of the drug from the swollen matrix. In most cases, drug release from polymeric formulations with swelling properties usually follows a non-Fickian (anomalous) pattern, but for macromolecules such as peptides and proteins, especially in the cases when there are significant interactions of ionic charges between the carrier polymer and the embedded moiety, the mechanism may be different. To elucidate the release mechanism of insulin (a peptide with considerable ionic charges) from the developed

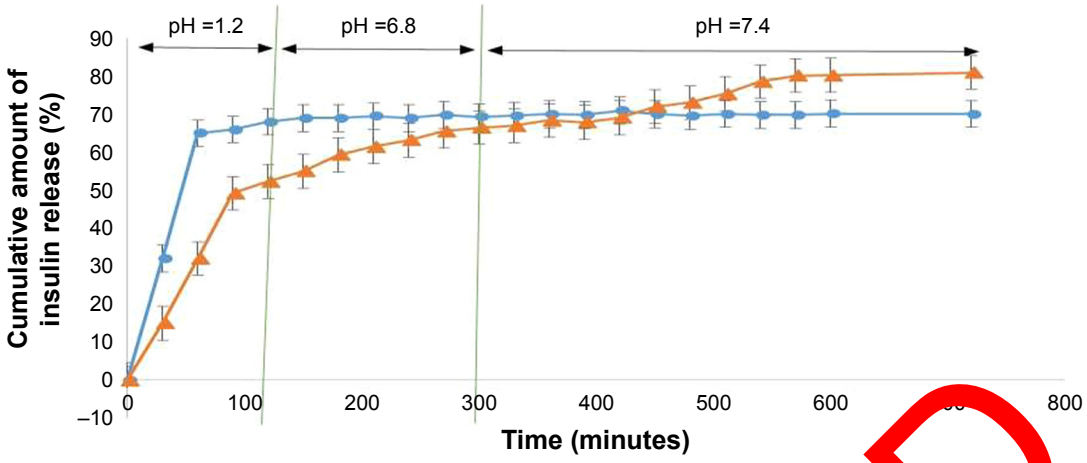

Figure 6 Insulin release profile of nanoparticles fabricated from native chitosan (Cs) and the new peptide-grafted derivative of Cs (CPP-g-Cs) at three different pH values.
Note: ●: Nanoparticles from Cs, ▲: nanoparticles from CPP-g-Cs.
Abbreviations: CPP, cell-penetrating peptide; Cs, chitosan.

NPs, the parameter "n" for Ritger–Peppas equation was investigated. The value for the correlation coefficient for the optimized formulation was found to be 0.8324 ($R \geq 0.99$); this obviously indicates that the release pattern is well fitted to the empirical equation. The "n" release exponent came out to be between 0.86 and 0.89, indicating a non-Fickian (anomalous) transport ($0.45 < n < 0.89$).

Hypoglycemic potential of the insulin-loaded NPs

Blood glucose level–time profiles following the administration of different insulin formulations to diabetic rats are depicted in Figure 7. As it is clear from the graph, after the oral administration of simple insulin powder filled in enteric protective capsules, no hypoglycemic effect is seen in diabetic rats, indicating the poor oral absorption of insulin without a suitable delivery system. Oral administration of insulin-loaded NPs from Cs filled in enteric coated capsule shows minimal but significant hypoglycemic effects ($P < 0.05$) and produced a nadir of around 18% after 3 hours, the hypoglycemic effect is sustained for 6 hours postadministration and then returned to base level. While insulin-loaded NPs from CPP-g-Cs filled in enteric-coated capsules presented a significant hypoglycemic effect and produced a reduction of around 30% in 4 hours postadministration and sustained this hypoglycemic effects up to 12 hours postadministration. As it is depicted in Figure 7, hypoglycemic effects from CPP-g-Cs NPs initiated around

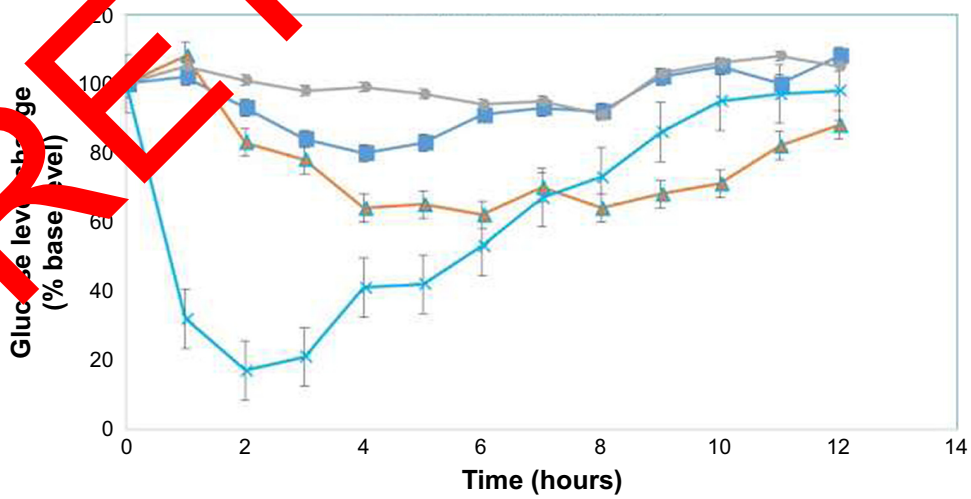

Figure 7 Glucose level changes (% base level) vs time profiles in diabetic rats following the administration of different formulations.
Note: ■: Insulin-loaded NPs from native Cs in enteric capsules (oral, 30 IU/kg); ▲: insulin-loaded NPs from CPP-g-Cs in enteric capsules (oral, 30 IU/kg); ●: simple insulin powder in enteric capsules (oral, 30 IU/kg); ×: simple insulin solution (SC, 5 IU/kg).
Abbreviations: CPP, cell-penetrating peptide; Cs, chitosan; CPP-g-Cs, peptide-grafted derivative of chitosan; NPs, nanoparticles; SC, subcutaneous.

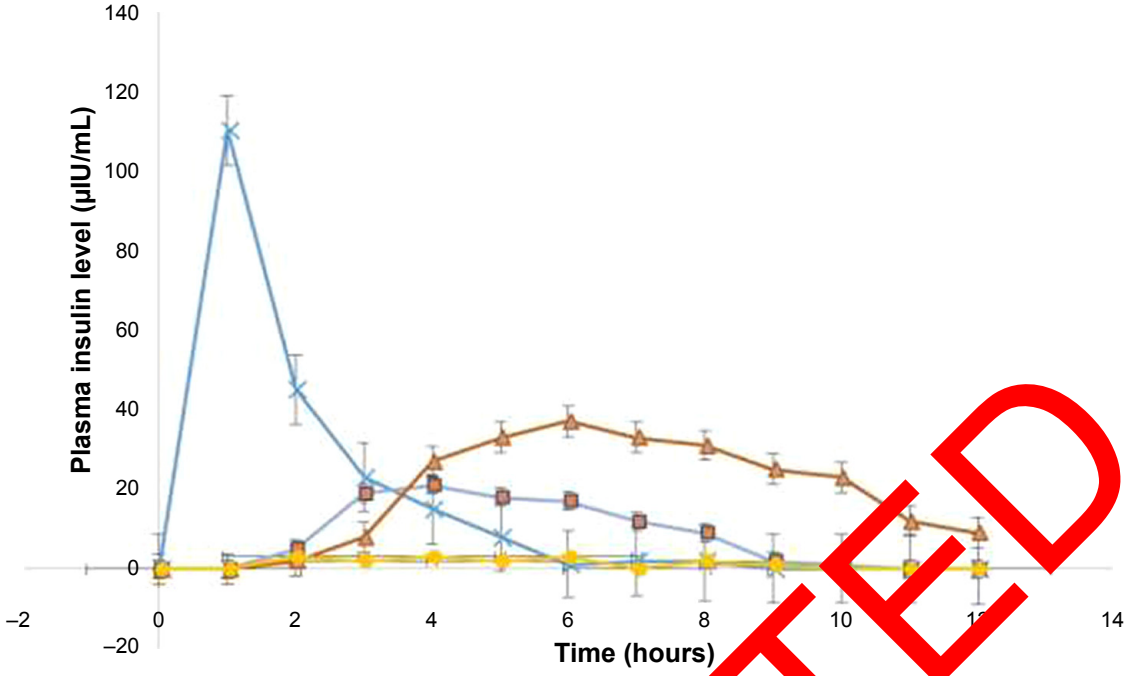

Figure 8 Plasma insulin level vs time profiles (μIU/mL) following the administration of different formulations.
Note: ×: Simple insulin solution (SC, 5 IU/kg); ■: insulin-loaded NPs from native Cs in enteric capsules (oral, 30 IU/kg); ▲: insulin-loaded NPs from CPP-g-Cs in enteric capsules (oral, 30 IU/kg); ●: simple insulin powder in enteric capsules (oral, 30 IU/kg).
Abbreviations: CPP, cell-penetrating peptide; Cs, chitosan; CPP-g-Cs, peptide-grafted derivative of chitosan; NPs, nanoparticles; SC, subcutaneous.

2 hours later than that of Cs NPs but are more pronounced and sustained much longer than hypoglycemic effects of Cs NPs. This phenomenon is consistent with the in vitro release behaviors of these two NPs in which Cs NPs showed a much higher burst release in the first 2 hours (63% and 47% for Cs and Cs-g-CPP NPs, respectively), but total release of insulin from Cs NPs is lower than that of CPP-g-Cs NPs (67% and 82% for Cs and Cs-g-CPP NPs, respectively). As expected, SC injection of insulin solution (5 IU/kg) produces a very sharp hypoglycemic effect in 2 hours after injection (~85% reduction in 2 hours postadministration), but remained effective for 5 hours postadministration and then returned sharply to baseline glucose level.

Plasma insulin concentration–time profiles and the corresponding pharmacokinetic (PK) parameters are shown in Figure 8 and Table 2, respectively. As depicted, the animals given SC injection (5 IU/kg) from simple solution of insulin showed a maximum plasma concentration (C_{max}=110.4±8 μIU/mL) at 1 hour after injection with sharp decrease afterward, whereas the animals treated with the oral administration of insulin-loaded NPs from Cs or CPP-g-Cs filled in enteric capsules showed different patterns; insulin-loaded NPs from Cs filled in enteric capsules showed a maximum plasma concentration (C_{max}) of 21.3±2.2 μIU/mL at 4 hours post-oral administration and sustained the developed level of insulin for 6 hours post-oral administration and then steadily decreased with mild slope resulting in an $AUC_{0-12\,h}$ of 103.6±4.1 μIU/mL.

For insulin-loaded NP fabricated from the CPP-g-Cs and filled in enteric capsules, maximum plasma concentration and the resulting $AUC_{0-12\,h}$ are much higher than that of NPs fabricated from simple Cs. C_{max} (37.6±3.2 μIU/mL) was achieved at 6 hours postadministration, and plasma insulin level remained considerably high for 10 hours and then

Table 2 PK parameters of insulin following the administration (oral or subcutaneous) of different formulations to diabetic rats

PK parameters	Simple insulin solution (SC)	Insulin-loaded NPs from Cs in enteric capsules	Insulin-loaded NPs from CPP-g-Cs in enteric capsules
Dose (IU/kg)	5	30	30
C_{max} (μIU/mL)	110.4±8	21.3±2.2	37.6±3.2
T_{max} (hours)	1	4	6
AUC (μIUh/mL)	220.8±5.3	103.6±4.1	259.3±6
BA_R (%)	100	7.8±0.7	19.6±1.3

Notes: PK parameters following the administration of three different formulations to diabetic rats: subcutaneous (SC) administration of simple insulin solution, oral administration of insulin-loaded NPs from chitosan filled in enteric protective capsules, and oral administration of insulin-loaded NPs from peptide-grafted derivative of chitosan (CPP-g-Cs) NPs filled in enteric protective capsules.
Abbreviations: AUC, area under the curve; BA_R, relative bioavailability; CPP, cell-penetrating peptide; Cs, chitosan; NPs, nanoparticles; PK, pharmacokinetic.

steadily began to decrease reaching around 9.3±1.2 µIU/mL at the end of 12 h experiment, leading to $AUC_{0-12\ h}$ of 259.3±6. As shown in Table 2, relative bioavailability of insulin resulting from the oral administration of insulin-loaded NP fabricated from native Cs is 7.8%±0.7%. This level of oral bioavailability for insulin resulting from the oral administration of insulin-loaded NPs from native Cs is consistent with the levels reported in other studies.[40,41] Cs is a mucoadhesive polymer and rich in positively charged amine groups that their electrostatic interactions with negatively charged sialic acid groups at the surface of intestinal cells offer effective adhesion and penetration of drug-loaded NPs or the released insulin into the luminal cells of intestine. Another special characteristic of Cs that is believed to be the reason for cell internalization is its potential to open the tight junctions between the intestinal cells offering a paracellular pathway for the penetration of large molecules and NPs.

For NPs developed from the CPP-g-Cs, in addition to mucoadhesion and tight-junction-opening characteristics of Cs, a new characteristic is added, and it is the direct cell penetration potential of the CPPs. This phenomenon gives the CPP or the cargo attached to it (chemically or physically) the potential to penetrate directly into the cells of all ... in a transcytosis model. In this study, the higher C_{max} and AUC for NPs from CPP-g-Cs in comparison with NPs fi... Cs can be attributed to the cell penetrati... potent...al of t... grafted CPP, providing the NPs from CP... g-Cs p... or with an additional mechanism for cell p...etratio... his added cell penetration potential for Cs N... containing ...PP tags was reported in our previous stu...y.[23]

As depicted in Fig... 8, maximu... plasma concentration of insulin result...g from the oral administration of NPs fabricated from CP... -Cs ...curs 6 hours postadministration, while the abs...tion o... insulin h... been initiated from 2 to 3 hours p... tadmi...stratio... h... considerable delay to reach to C_{max} ...n be hy...thesized to the reason that NPs containing CPP tags ...be taken up into the cells as a whole particle embedding n...erous insulin molecules before disintegration of NP (due to cargo delivery potential of CPP[42,43]), ie, following the penetration of every single NP, is internalized into the cells, and release of insulin from the NPs continues inside the epithelial cells or inside general circulation, increasing cumulative release of insulin and reaching to C_{max} once enough insulin-loaded NPs are internalized and release their embedded insulin inside general circulation. This phenomenon was investigated in a Caco-2 cell study in our previous report.[23]

Conclusion

In this study, a novel CPP-g-Cs was synthesized, and the successful attachment of the special peptide (CPP) was investigated through FTIR and ^{1}H NMR studies. The new derivative is freely water-soluble even in neutral and alkaline pH. Insulin-loaded NPs from this polymer exhibit desired particle size, drug loading, and drug release behavior for insulin and possibly other peptide and protein drugs. Following the oral administration of insulin-loaded NPs to diabetic rats, the relative bioavailability was 19.6%, and the hypoglycemic effect sustained for a... 10 hours. This novel derivative of Cs has a great pr...ise for t... oral delivery of proteins and peptides and ca... further opt...ized through applying other CPPs or ...hanging ...e degre... of substitution in Cs polymer.

Disclosu...

The author... report no co...icts ... interest in this work.

References

1. ...baş EB, Odabaş... Chitosan microspheres and sponges: preparation and characterization. *J Appl Polym Sci*. 2000;76(11):1637–1643.
2. Anitha A, ...epa N, Chennazhi K, Nair S, Tamura H, Jayakumar R. Developme... of mucoadhesive thiolated chitosan nanoparticles for biomedical ...pplications. *Carbohydr Polym*. 2011;83(1):66–73.
3. ... Powers K, Baney R. Physicochemical properties and blood compatibility of acylated chitosan nanoparticles. *Carbohydr Polym*. ...04;58(4):371–377.
4. Chen J, Huang L, Lai H, et al. Methotrexate-loaded PEGylated chitosan nanoparticles: synthesis, characterization, and in vitro and in vivo antitumoral activity. *Mol Pharm*. 2013;11(7):2213–2223.
5. Friedman AJ, Phan J, Schairer DO, et al. Antimicrobial and anti-inflammatory activity of chitosan–alginate nanoparticles: a targeted therapy for cutaneous pathogens. *J Invest Dermatol*. 2013;133(5):1231–1239.
6. Li LH, Deng JC, Deng HR, Liu ZL, Li XL. Preparation, characterization and antimicrobial activities of chitosan/Ag/ZnO blend films. *Chem Eng J*. 2010;160(1):378–382.
7. Xia W, Liu P, Zhang J, Chen J. Biological activities of chitosan and chitooligosaccharides. *Food Hydrocoll*. 2011;25(2):170–179.
8. Skaugrud Ø, Hagen A, Borgersen B, Dornish M. Biomedical and pharmaceutical applications of alginate and chitosan. *Biotechnol Genet Eng Rev*. 1999;16(1):23–40.
9. Ilium L. Chitosan and its use as a pharmaceutical excipient. *Pharm Res*. 1998;15(9):1326–1331.
10. Yeh TH, Hsu LW, Tseng MT, et al. Mechanism and consequence of chitosan-mediated reversible epithelial tight junction opening. *Biomaterials*. 2011;32(26):6164–6173.
11. Vllasaliu D, Exposito-Harris R, Heras A, et al. Tight junction modulation by chitosan nanoparticles: comparison with chitosan solution. *Int J Pharm*. 2010;400(1):183–193.
12. Wong CY, Al-Salami H, Dass CR. Potential of insulin nanoparticle formulations for oral delivery and diabetes treatment. *J Control Release*. 2017;264:247–275.
13. Ismail R, Csóka I. Novel strategies in the oral delivery of antidiabetic peptide drugs-insulin, GLP 1 and its analogs. *Eur J Pharm Biopharm*. 2017;115:257–267.
14. Li L, Jiang G, Yu W, et al. Preparation of chitosan-based multifunctional nanocarriers overcoming multiple barriers for oral delivery of insulin. *Mater Sci Eng C Mater Biol Appl*. 2017;70(Pt 1):278–286.

15. Ross PL, Milburn J, Reith DM, Wiltshire E, Wheeler BJ. Clinical review: insulin pump-associated adverse events in adults and children. *Acta Diabetol*. 2015;52(6):1017–1024.
16. Goldberg M, Gomez-Orellana I. Challenges for the oral delivery of macromolecules. *Nat Rev Drug Discov*. 2003;2(4):289–295.
17. Khafagy ES, Morishita M, Onuki Y, Takayama K. Current challenges in non-invasive insulin delivery systems: a comparative review. *Adv Drug Deliv Rev*. 2007;59(15):1521–1546.
18. Aguirre TA, Teijeiro-Osorio D, Rosa M, Coulter IS, Alonso MJ, Brayden DJ. Current status of selected oral peptide technologies in advanced preclinical development and in clinical trials. *Adv Drug Deliv Rev*. 2016;106(Pt B):223–241.
19. Li L, Jiang G, Yu W, et al. A composite hydrogel system containing glucose-responsive nanocarriers for oral delivery of insulin. *Mater Sci Eng C Mater Biol Appl*. 2016;69:37–45.
20. Shan W, Zhu X, Tao W, et al. Enhanced oral delivery of protein drugs using zwitterion-functionalized nanoparticles to overcome both the diffusion and absorption barriers. *ACS Appl Mater Interfaces*. 2016; 8(38):25444–25453.
21. Salamat-Miller N, Chittchang M, Johnston TP. The use of mucoadhesive polymers in buccal drug delivery. *Adv Drug Deliv Rev*. 2005;57(11): 1666–1691.
22. Déat-Lainé E, Hoffart V, Garrait G, et al. Efficacy of mucoadhesive hydrogel microparticles of whey protein and alginate for oral insulin delivery. *Pharm Res*. 2013;30(3):721–734.
23. Barbari GR, Dorkoosh FA, Amini M, et al. A novel nanoemulsion-based method to produce ultrasmall, water-dispersible nanoparticles from chitosan, surface modified with cell-penetrating peptide for oral delivery of proteins and peptides. *Int J Nanomedicine*. 2017;12:3471–3483.
24. Kamei N, Morishita M, Eda Y, Ida N, Nishio R, Takayama K. Usefulness of cell-penetrating peptides to improve intestinal insulin absorption. *J Control Release*. 2008;132(1):21–25.
25. Deshayes S, Morris MC, Divita G, Heitz F. Cell-penetrating peptide tools for intracellular delivery of therapeutics. *Cell Mol Life Sci*. 200 62(16):1839–1849.
26. Endoh T, Ohtsuki T. Cellular siRNA delivery using cell-penetrating peptides modified for endosomal escape. *Adv Drug Deliv Rev*. 2009; 61(9):704–709.
27. Heitz F, Morris MC, Divita G. Twenty years of cell-penetrating peptides: from molecular mechanisms to therapeutics. *Br J Pharmacol*. 2009;157(2):195–206.
28. Zorko M, Langel Ü. Cell-penetrating peptides: mechanism and kinetics of cargo delivery. *Adv Drug Deliv Rev*. 2005;57(4):529–545.
29. Khafagy el-S, Kamei N, Nielsen EJ, Nishio R, Takeda-Morishita M. One-month subchronic toxicity study of cell-penetrating peptides for insulin nasal delivery in rats. *Eur J Pharm Biopharm*. 2013;85(3 Pt A): 736–743.
30. Kitchens KM, Kolhatkar RB, Swaan PW, Eddington ND, Ghandehari H. Transport of poly(amidoamine) dendrimers across Caco-2 cell monolayers: influence of size, charge and fluorescent labeling. *Pharm Res*. 2006;23(12):2818–2826.
31. Home PD, Barriocanal L, Lindholm A. Comparative pharmacokinetics and pharmacodynamics of the novel rapid-acting insulin analogue, insulin aspart, in healthy volunteers. *Eur J Clin Pharmacol*. 1999;55(3): 199–203.
32. Chen CC, Rajagopal B, Liu XY, et al. A mild removal of Fmoc group using sodium azide. *Amino Acids*. 2014;46(2):367–374.
33. Sonaje K, Chen YJ, Chen HL, et al. Enteric-coated capsules filled with freeze-dried chitosan/poly (γ-glutamic acid) nanoparticles for oral insulin delivery. *Biomaterials*. 2010;31(12):3384–3394.
34. Hakim L, Sabarudin A, Oshima M, Motomizu S. Synthesis of novel chitosan resin derivatized with serine diacetic acid moiety and its application to on-line collection/concentration of trace elements and their determination using inductively coupled plasma-atomic emission spectrometry. *Anal Chim Acta*. 2007; (1):73–81.
35. Gan Q, Wang T, Cochrane C, McCarron P. Modulation of surface charge, particle size and morphological properties of chitosan–TPP nanoparticles intended for gene delivery. *Colloids Surf B Biointerfaces*. 2005;44(2–3):65–73.
36. Fan W, Yan W, Xu Z, Ni H. Formation mechanism of monodisperse, low molecular weight chitosan nanoparticles by ionic gelation technique. *Colloids Surf B Biointerfaces*. 2012; :27.
37. Avadi MR, Sadeghi M, Mohammadpour N, et al. Preparation and characterization of insulin nanoparticles using chitosan and Arabic gum with ionic gelation method. *Nanomedicine*. 2010;6(1):58–63.
38. Qin C, Li H, Xiao Q, Liu Y, Zhu J, Du Y. Water-solubility of chitosan and its antimicrobial activity. *Carbohydrate Polymers*. 2006;63(3): –374.
39. Mukhopadhyay P, Kundu PP. Chitosan-graft-PAMAM–alginate core–shell nanoparticles: a safe and promising oral insulin carrier in an animal model. *RSC Adv*. 2015;5(114):93995–94007.
40. Sarmento B, Ribeiro A, Veiga F, Sampaio P, Neufeld R, Ferreira D. Alginate/chitosan nanoparticles are effective for oral insulin delivery. *Pharm Res*. 2007;24(12):2198–2206.
41. Anand P, Nair HB, Sung B, et al. RETRACTED: Design of curcumin-loaded PLGA nanoparticles formulation with enhanced cellular uptake, and increased bioactivity in vitro and superior bioavailability in vivo. *Biochem Pharmacol*. 2010;79(3):330–338.
42. Hällbrink M, Florén A, Elmquist A, Pooga M, Bartfai T, Langel Ü. Cargo delivery kinetics of cell-penetrating peptides. *Biochim Biophys Acta*. 2001;1515(2):101–109.
43. Wang F, Wang Y, Zhang X, Zhang W, Guo S, Jin F. Recent progress of cell-penetrating peptides as new carriers for intracellular cargo delivery. *J Control Release*. 2014;174:126–136.